Oligogermanes and related silicon and tin containing germanes: structure, optical and semiconductor properties

Kirill V. Zaitsev,*[a] Viktor A. Tafeenko,[a] Yuri F. Oprunenko,[a] Anastasia V. Kharcheva,[a] Zhaisan Zhanabil,[b] Yerlan Suleimen,[b] Kevin Lam,*[b] Vladimir B. Zaitsev,[c] and Anna V. Zaitseva[d]

Abstract: The optical (UV/vis absorbance, fluorescence in solid state and in solution) and semiconducting properties of a number of di- and trigermanes and related silicon and tin containing germanes, **1**-**6** ((*p*-Tol)$_3$GeGeMe$_3$ (**1**), (Ph$_3$SnGe(SiMe$_3$)$_3$ (**2**), (C$_6$F$_5$)$_3$GeGePh$_3$ (**3**), (*p*-Tol)$_3$GeSiMe$_2$SiMe$_3$ (**4**), (*p*-Tol)$_3$GeGeMe$_2$Ge(*p*-Tol)$_3$ (**5**), (*p*-Tol)$_3$GeSiMe$_2$SiMe$_2$Ge(*p*-Tol)$_3$ (**6**)) were investigated. Molecular structures of **5** and **6** were studied by X-ray diffraction analysis. All compounds displayed luminescence properties. In addition, a band gap (of about 3.3 eV) was measured for the compounds **1**-**6** showing that that those molecules display semiconductor properties.

Introduction

Catenated oligosilanes[1] and oligogermanes[2] are attracting more and more the attention of the scientific community due to their unique physical properties. These compounds possess strong UV/visible absorption, luminescence, photo- and electric conductivity due to presence of an effective σ-conjugation between the Group 14 elements (E = Si, Ge, Sn, Pb). A special attention should be paid to germanium compounds since they exhibit semiconducting properties due to their smaller band gap and higher electron and hole mobility.

Semiconducting properties in polymeric catenated Group 14 derivatives are usually observed after the molecule has undergone a doping process by SbF_5 or AsF_5.[3] In this case a partial oxidation results in the formation of a cation-radical, similar to the "hole" usually found in elemental Si or Ge, and leads to a positive charge mobility within the elemental chain itself. In fact, polygermanes/polysilanes intrinsically display photoconductivity in which the electron transport is assured by a hole hopping process. Such as phenomenon strongly depends on the nature and on the length of the side-chain.[4] The construction of semiconducting devices based on such polymer materials[5] (polysilanes, polygermanes, polystannanes) relies on specific techniques, such as the production of doped thin films.[6] Interestingly, the band gap in Ge is lower than the one in Si and hence one could expect enhanced conductive properties in individual germanium organic compounds. Therefore, the synthesis and the studies of the shortest Group 14 element chain (especially containing Ge atoms) which is necessary for the conductive properties to be observed may be regarded as an essential task in the development of new semiconducting devices based on germanium. The conductivity mechanism in free oligogermanes and related compounds is significantly different from the one observed in other related conductive materials due to σ-bond electrons delocalization.[7] In oligogermanes, it is well known that the HOMO is distributed across the chain of Group 14 elements and an interchain hopping mechanism has been previously described.

Investigations and studies of small molecules and their properties should help to establish a "structure–property" relationship. Recently, several works emerged in which single-molecule conductance has been studied.[8] But in such studies a very specific and complex method (scanning tunneling microscope-based break-junction) was used to measure the conductance.

Taking into account that oligogermanes as well as related silicon and tin containing germanes include semiconducting (silicon and germanium) atoms, we decided to investigate the optical and semiconductor properties of several molecular organometallic compounds (**1-6**) in their solid state. The optical and electrochemical properties of oligogermanes were also investigated in solution.

Results and Discussion

Germanes **1**, **2**[9] and **3**[10] were prepared using known procedures. Compounds **4-6** were prepared by reacting (*p*-Tol)$_3$GeLi, formed *in situ*, with a silicon or germanium halide (Scheme 1).

[a] Dr. Kirill V. Zaitsev, Dr. Viktor A. Tafeenko, Dr. Yuri F. Oprunenko, Anastasia V. Kharcheva
Department of Chemistry
Moscow State University
Leninskye Gory, 1, 3, Moscow 119991, Russia
E-mail: zaitsev@org.chem.msu.ru
[b] Zhaisan Zhanabil, Dr. Yerlan Suleimen, Dr. Kevin Lam
Department of Chemistry
School of Science and Technology, Nazarbayev University
Astana, Kazakhstan, 010000
E-mail: kevin.lam@nu.edu.kz
[c] Dr. Vladimir B. Zaitsev
Department of Physics
Moscow State University
Leninskye Gory, 1, Moscow 119991, Russia
[d] Dr. Anna V. Zaitseva
Institute of Physical Chemistry
Russian Academy of Sciences
Leninskii pr. 31, Moscow, Russia

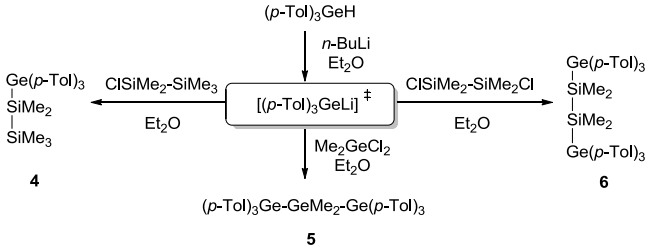

Scheme 1. Synthesis of compounds **4**-**6**.

Compounds **4-6** were isolated in good yields as white crystalline air and moisture stable powder, soluble in common organic solvents (toluene, ether, chloroform, THF).

The structures of compounds **5** and **6** in solid state were studied by X-ray analysis (Figures 1 and 2; Table S1, Supporting Information); in solution, the structures of those novel derivatives were investigated by multinuclear NMR (see Supporting Information, Figures S1-S11), UV/vis and emission spectroscopies as well as by electrochemistry. For comparison purposes, the luminescent properties of compounds **1-3** were also studied.

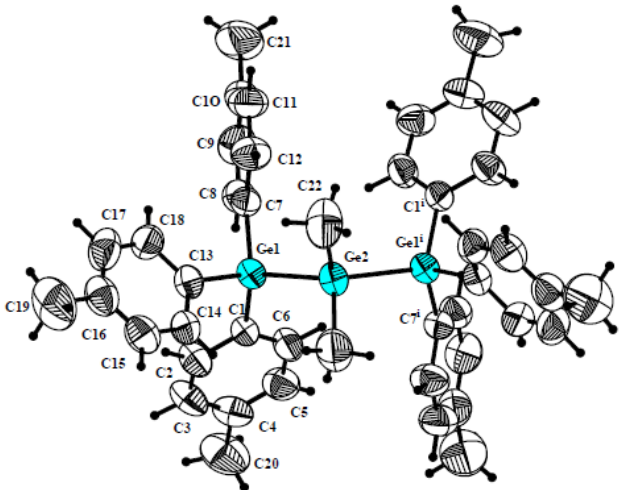

Figure 1. Molecular structure of **5**. Displacement ellipsoids are shown at 50% probability level. Selected bond lengths (Å) and bond angles (deg): Ge-Ge 2.4219(6), Ge(1)-C_{av} 1.949(4), Ge(2)-C(22) 1.941(5); C-Ge(1)-C_{av} 108.39(19), C-Ge(1)-Ge(2)$_{av}$ 110.46(12), C(22)-Ge(2)-C(22i) 106.5(4), C-Ge(2)-Ge(1)$_{av}$ 107.32(17), Ge(1)-Ge(2)-Ge(1i) 120.37(4).

To the best of our knowledge, only 10 structures of linear trigermanes have been reported so far (Table 1). The steric hindrance and the electronic properties of the substituents (electron donors or acceptors) are the main factors that impact the structural parameters of oligogermanes.

The crystal structure of compound **5** is highly symmetric and displays a C_{2v} symmetry. Geometry at each Ge atom may be described as a slightly distorted tetrahedron. The substituents at the neighboring Ge atoms are in an *anti*-conformation (the average value of torsion angle C-Ge(1)-Ge(2)-C is 175.76(19)º). The value of Ge(1)-Ge(2)-Ge(1i) (120.37(4)º) angle is close to 120º,[18] which indicates an efficient delocalization of σ-electron density between the Ge atoms. In general the structural parameters of **5** are very close to those of (*p*-Tol)$_3$Ge-GeMe$_3$, **1**.[9] At the same time, **5** displays the shortest Ge-Ge bond length among the known trigermanes investigated by X-ray analysis.

Table 1. The main structural parameters of trigermanes investigated by X-ray analysis.

Trigermane	*d*(Ge-Ge)$_{av}$, Å	Angle Ge-Ge-Ge$_{av}$, deg	Angle C-Ge$_{central}$-C$_{av}$, deg	Reference
[Ph$_3$Ge]$_2$GePh$_2$	2.440(2)	121.3(1)	108.7(4)	[11]
[Ph$_3$Ge]$_2$GeMe$_2$	2.429(1)	120.3(1)	109.2(2)	[12]
[ClPh$_2$Ge]$_2$GePh$_2$	2.423(4)	113.52(12)	111.82(13)	[13]
[Me(*t*-Bu)$_2$Ge]$_2$Ge(*t*-Bu)$_2$	2.620(3)	118.56(17)	110.31(15)	[14]
[Br(*t*-Bu)$_2$Ge]$_2$Ge(*t*-Bu)$_2$	2.609(2)	113.61(15)	109.25(12)	[14]
[I(*t*-Bu)$_2$Ge]$_2$Ge(*t*-Bu)$_2$	2.641(1)	115.38(10)	109.36(12)	[15]
[(*p*-Tol)$_3$Ge]$_2$GePh$_2$	2.4328(5)	114.80(2)	106.2(1)	[16]
[(*p*-Tol)$_3$Ge]$_2$Ge(*p*-Tol)$_2$	2.4404(5)	117.54(1)	106.45(9)	[16]
[(*p*-Tol)$_3$Ge]$_2$Ge(C$_6$F$_5$)$_2$	2.459(5)	124.10(3)	108.0(2)	[10]
[(Me$_3$Si)$_3$Ge]$_2$GeMe$_2$	2.4616(8)	125.00(4)	105.35(6)	[17]
[(*p*-Tol)$_3$Ge]$_2$GeMe$_2$	2.4219(6)	120.37(4)	106.5(4)	this work

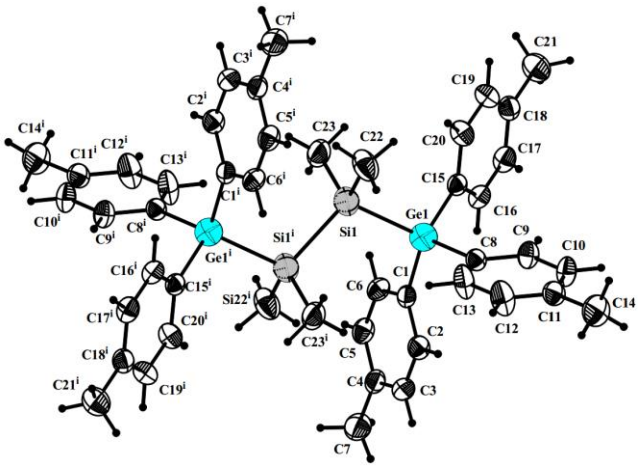

Figure 2. Molecular structure of **6**. Displacement ellipsoids are shown at 50% probability level. Selected bond lengths (Å) and bond angles (deg): Ge(1)-Si(1) 2.3972(10), Si(1)-Si(1i) 2.3486(18), Ge(1)-C_{av} 1.952(3), Si(1)-C_{av} 1.871(3); C-Ge(1)-C_{av} 107.29(13), C-Ge(1)-Si(1)$_{av}$ 111.56(9), C(22)-Si(1)-C(23) 108.6(2), C-Si(1)-C_{av}109.77(14), C(22)-Si(1)-Ge(1) 108.51(14), Si(1i)-Si(1)-Ge(1) 110.31(5).

Molecular structure of compound **6** is centrosymmetric (space group *P-1*, Z= 1). The structural parameters are very close to those found for $(p\text{-Tol})_3Ge\text{-}SiMe_3$.[9] In **6**, the substituents along the Ge-Si bond in $(p\text{-Tol})_3\mathbf{Ge\text{-}Si}Me_2$ fragment are in a skewed conformation[18b] (torsion angle C-Ge-Si-C is 86.58(14)°). At the same time the geometry along $Me_2\mathbf{Si\text{-}Si}Me_2$ fragment may be described as an ideal *anti*-conformation (torsion angle Ge-Si-Si-Ge is 180.00(5)º). Such a conformation allows for an effective σ-conjugation in the chain of four atoms of Group 14 elements.

Only three compounds with a related structure have been reported so far (Table 2).

Table 2. Structural parameters of compounds with Ge-Si-Si-Ge chain.

Compound	*d*(Ge-Si)$_{av}$, Å	*d*(Si-Si), Å	Angle Ge-Si-Si, deg	Torsion Ge-Si-Si-Ge, deg	reference
$[K(Me_3Si)_2Ge\text{-}SiMe_2\text{-}]_2$*2[18-crown-6]	2.429(2)	2.378(3)	116.05(10)	180	[19]
$[(Me_3Si)_3Ge\text{-}SiMe_2\text{-}]_2$	2.407(2)	2.379(2)	116.23(8)	180	[20]
$[(Me_3Ge)_3Ge\text{-}SiMe_2\text{-}]_2$	2.410(2)	2.349(3)	114.81(5)	180	[17]
6	2.397(1)	2.349(2)	110.31(5)	180	this work

When comparing the structural parameters of **6** with the related compounds showed in Table 2 it is evident that the steric volume of the substituents plays a key role in the geometry of such molecules. Introduction of bulky groups, even at the ends of the elemental chain leads to a noticeable increase in bond lengths.

The chemical shifts in NMR spectra of related *p*-tolyl substituted Ge and Si derivatives **4-6** are very similar. Thus in ^{1}H NMR there are two doublets in aromatic field (at δ 7.32-7.18 and 7.15-7.03 ppm with 7.8 Hz spin coupling constant) and singlet of methyl group (at approximately δ 2.35 ppm). Very similar signals of *C*H groups are observed in ^{13}C NMR (at approximately δ 135.4, 128.9 ppm) typical for *para*-substituted tolyl group but the *ipso*-carbons (at δ 137.9 and 134.6-135.2 ppm) are more sensitive to the nature of substituent.

The topology of the single crystal surface of compounds **1**, **2** and **5** was investigated by AFM. Figures 3 and 4 show the AFM data for compound **1** (for other compounds see Supporting Information, Figures S12-S17).

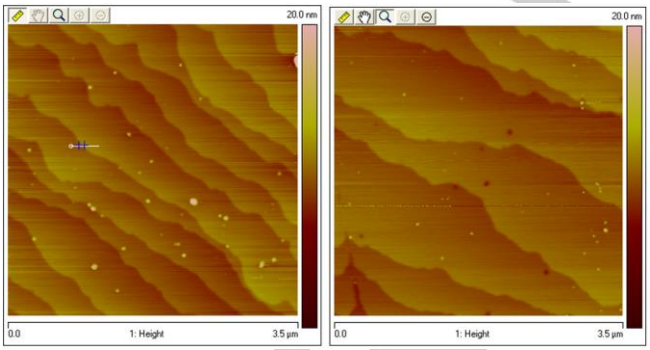

Figure 3. AFM image of different regions of compound **1**, single crystal surface.

As it can be seen from Figure 3, the corresponding growth steps may be easily measured. Plotting of surface cross-sections allows estimating the height of these growth steps. Figure 4, shows an analysis of compound **1** surface profile for one of the investigated sites.

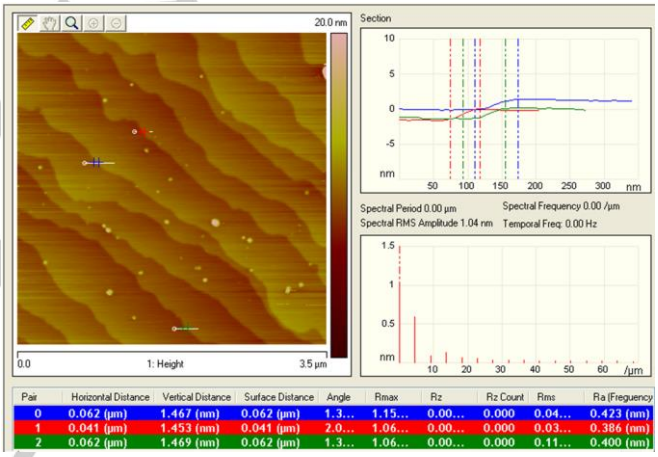

Figure 4. AFM image of the surface of compound **1** single crystal and three surface profile cross-sections.

The analysis of cross-sections obtained with several samples of the same compound, provides an average value of 1.46 ± 0.01 nm for the step height growth. Such a value correlates with the size of elemental cell (a:b:c= 10.6888(2):19.3569(4):12.2900(3) Å) of **1** according to X-ray.[9] In the case of **2** the step height growth is 0.97± 0.03 nm.

The UV/vis absorbance spectra of compounds **4-6** in solution are given in Figure 5.

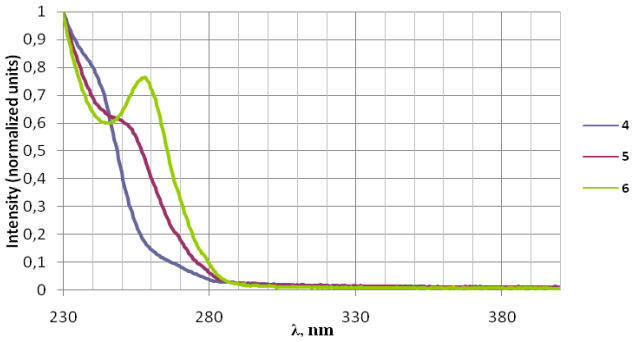

Figure 5. UV/vis absorption spectra (normalized) for **4-6** in CH_2Cl_2.

The data concerning UV/vis absorption of **4**-**6** and related compounds are given in Table 3.

Table 3. UV/visible absorption for **4**-**6** and related compounds.

Compound	λ_{max}, nm ($\varepsilon \times 10^{-4}$, $M^{-1}cm^{-1}$)	reference
$Me_3Si\text{-}SiMe_2\text{-}SiMe_3$	217 (0.8)	[21]
$Me_3Ge\text{-}GeMe_2\text{-}GeMe_3$	218 (0.8)	[22]
$PhMe_2Si\text{-}SiMe_2\text{-}SiMe_2Ph$	243 (1.95)	[23]
$Ph_3Si\text{-}SiPh_2\text{-}SiPh_3$	254 (3.22)	[23]
(p-Tol)$_3$Ge-$SiMe_2$-$SiMe_3$ (**4**)	241 (2.5)	this work
(p-Tol)$_3$Ge-$SiMe_2$-$SiMe_2$-Ge(p-Tol)$_3$ (**6**)	258 (4.7)	this work
$Ph_3Ge\text{-}GeEt_2\text{-}GeEt_2\text{-}GePh_3$	256 (4.60)	[24]
$Ph_3Ge\text{-}GePh_2\text{-}GePh_2\text{-}GePh_3$	282 (4.5)	[11]
(p-Tol)$_3$Ge-$GePh_2$-$GePh_2$-Ge(p-Tol)$_3$	285	[16]
$Ph_3Ge\text{-}GeMe_2\text{-}GePh_3$	245 (3.02)	[24]
$Ph_3Ge\text{-}SiMe_2\text{-}GePh_3$	244 (4.42)	[24]
$Ph_3Ge\text{-}GePh_2\text{-}GePh_3$	250 (4.42)	[24]
$Ph_3Ge\text{-}Ge(Me)Ph\text{-}GePh_3$	250 (4.56)	[24]
(p-Tol)$_3$Ge-$GeMe_2$-Ge(p-Tol)$_3$ (**5**)	251 (4.0)	this work
(p-Tol)$_3$Ge-$GePh_2$-Ge(p-Tol)$_3$	251 (3.17)	[16]
(p-Tol)$_3$Ge-Ge(p-Tol)$_2$-Ge(p-Tol)$_3$	253 (2.55)	[16]
(p-Tol)$_3$Ge-Ge(C_6F_5)$_2$-Ge(p-Tol)$_3$	258 (1.4)	[10]

Looking at the data obtained, it is evident that the substitution of a silicon atom by a germanium results in a red shift of the absorption band of the molecule. This could be explained by an effective conjugation between the identical atoms in the chain. A more significant shift is observed in the presence of aromatic substituents at Ge or Si centers.[10, 24-25] Increasing the number of atoms in the chain also resulted in a bathochromic shift. Furthermore, in the case of compound **6** the absorption band is clearly visible and may be due to an ideal conjugated structure similar to the one found in the crystal. At the same time, the nature of the substituting groups located at the end and in the centre of the linear molecule clearly showed to impact on the UV/vis absorption. On the one hand, electron donating groups such as *p*-tolyl (when compared with phenyl) present at the ends of the chain resulted in a bathochromic shift. On the other hand, electron withdrawing groups such as perfluorophenyl (when compared with methyl or phenyl) lead to an even more significant red shift. Substitution on the central Ge atom (Me, Ph or *p*-Tol) has only a small effect on the absorption properties of the molecule. In conclusion, in solution, the substitution in the chains of Group 14 elements results in better conjugation between these atoms and in a bathochromic shift in UV/vis absorption.

When moving from solution to the solid state, the studied compounds showed new optical properties. The absorption bands not only start at longer wavelengths but also display the characteristic shape of semiconductor absorption bands. The Kubelka–Munk plot for compound **3** is shown on Figure 6.

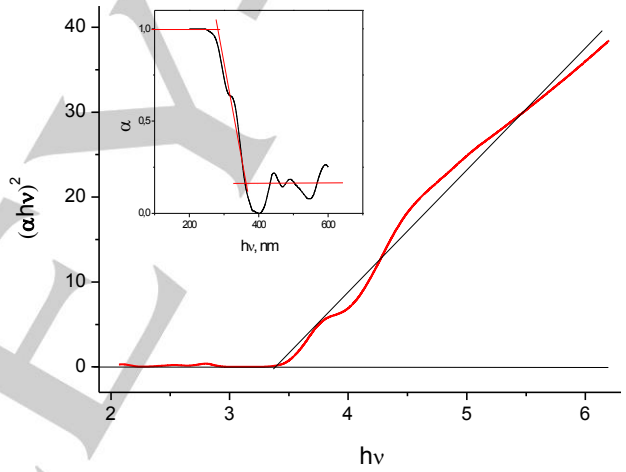

Figure 6. The plot of Kubelka–Munk function derivative for compound **3** used for the optical band gap E_g calculation. **Insert:** spectral dependence of the absorption coefficient of compound **3** in solid state.

From this spectral dependence it is seen that a threshold wavelength exists below which, the absorbance increases dramatically. Since the solid state samples were powders or single crystals the absorption spectra were recalculated from measured diffuse reflection.

The optical band gap energy E_g of the solid samples was determined from the so-called intrinsic absorption edge. Several methods exist to accomplish this. The first method allowed us to make an approximate estimate of E_g directly from the plot of the absorption coefficient α. At high λ, the energy of a quantum is small and no absorption occurs. This corresponds to the right part of the curve shown in the insert at Figure 6. Once λ attains the critical value of λ_{edge}, the absorption abruptly rises. This means that a sharp kink of the α(λ) dependence occurs at $\lambda = \lambda_{edge}$ (see Figure 6 insert). The energy of a light quantum is related to the wavelength as $E = hc/\lambda = h\nu$.

The main drawback of this approach lies in the difficulty to estimate correctly the absorption coefficient from scattering spectra. The α value of semiconductor materials varies within a wide range from 10^{-2} to 10^{5} cm^{-1}. For this reason, when the absorption coefficient is measured, the thickness of a specimen is selected in such a manner that the absorbance $D = \alpha d$ (where d is the thickness of a specimen) is nearly equal to 1. In this case, it is possible to use, with an admissible error, the expression

$$T\,(1 - R)^2 = \exp(-D),$$

which allow calculating the absorption coefficient from the measured R (Fresnel reflection coefficient), T (transmittance), and d as

$$\alpha = \frac{1}{d} ln \frac{(1-R)^2}{T}$$

The situation becomes more complex for the detection of scattered radiation. Although no strict multiple scattering theory exists, the theory of the diffuse reflection and transmission of optically opaque specimens, *i.e.*, the so-called two-component theory developed by Kubelka and Munk, is rather widely applied. For scattering specimens, this theory has the same importance as the Bouguer–Beer law in the absorption spectroscopy of transparent specimens. In Kubelka-Munk theory, it is assumed that reflected radiation is isotropic, *i.e.*, direction independent, and radiating light is monochromatic. As a result of the solution of the Kubelka–Munk equation system, it turns out that the diffuse reflectance R_∞ of a specimen depends only on the ratio of the absorption coefficient α and the scattering coefficient S instead of either the scattering coefficient or the absorption coefficient, i.e.,

$$\alpha/S = (1 - R_\infty)^2/2R_\infty = F(R_\infty)$$

The function $F(R_\infty)$ is called the Kubelka–Munk function. In diffuse reflection spectroscopy, as well as in absorption and emission spectroscopy, the dependence of the response of an instrument on the wavelength must be eliminated. This is provided by measuring the diffuse reflection spectrum of a specimen itself $\log R(\lambda)$ and the spectrum of scattering from an infinitely reflecting surface $R_{ref}(\lambda)$, for instance, from a surface coated with a thin barium sulfate, magnesium carbonate, or magnesium oxide layer; here, the ratio is calculated in the logarithmic form $\log[R(\lambda)/R_{ref}(\lambda)]$. In the absence of reflection from the bottom part of a specimen (for example, when a specimen has a sufficient thickness for the light to be completely absorbed), it is equal to $\log R_\infty$. For the practical estimation of the band gap energy in the case of direct interband transitions, the experimental data are expressed in the form of the dependence

$$(\alpha h\nu)^2 = A^2(h\nu - E_g),$$

which must be linear (Figure 6). As can be seen from Figure 6, the value of E_g is determined by extrapolating the linear dependence to the intersection with the abscissa axis.

The experimental dependence of α with hν for indirect interband transitions are plotted in the form of curves $\sqrt{\alpha} = f(h\nu)$.

We analyzed the results using a variety of methods for determining the width of the forbidden zone. All our results proved that compounds **1**–**6** possess semiconductor properties. The values of band gap for those materials were in average 3.3 ± 0.1 eV. According to DFT calculations for semiconductor polymers $[Ph_2Ge]_n$ the bandgap width is 2.13 eV.[26] Furthermore, partial substitution of phenyl groups by protons, *i.e.* $[Ph(H)Ge]_n$ and $[H_2Ge]_n$, results in 2.72 and 3.03 eV bandgap width. This reveals the critical role of aryl groups (σ-π conjugation) in the bandgap width value. The comparison with related silicon derivatives, $[Ph_m(H)_{2-m}Si]_n$, gives 3.61 (m = 2), 3.72 (m = 1) and 4.53 (m = 0) eV,[27] or 3.5 eV for $[MePhSi]_n$[7] reflects the role of the nature of the catenated atom in the chain.[9] Therefore we are confident that molecular oligogermanes, due to their physical properties are promising semiconducting precursors.

In semiconducting organometallic compounds such as **1**–**6** the band gap is determined by the HOMO/LUMO gap. Decrease of the energy gap by varying the nature of the substituents (introduction of only electron withdrawing substituents,[10] or only electron donating groups, substitution by Sn atoms[9] or increasing the number of catenated atoms in the chain) should result in the apparition of bulk semiconductor properties.

The luminescent properties of compounds **2**–**6** were studied (Table 5) in solution (Figure 7) and in solid state (Figures 8–9, Figure S18, Supporting Information).

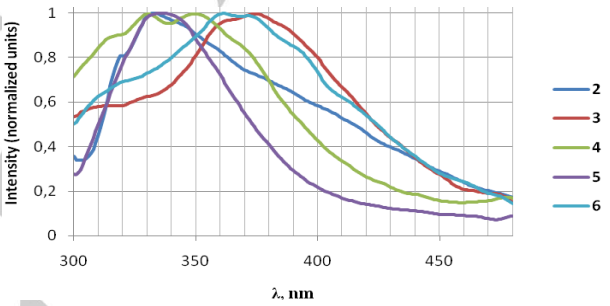

Figure 7. Emission spectra of compounds **2**–**6** in solition in CH_2Cl_2.

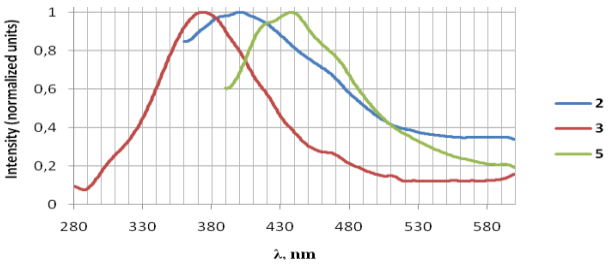

Figure 8. Emission spectra of compounds **2**, **3** and **5** in solid state.

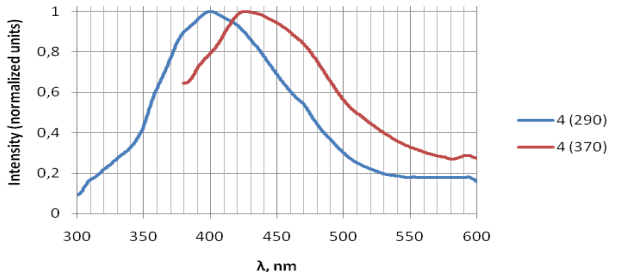

Figure 9. Emission spectra of compound **4** in solid state at different exitation.

Table 5. Fluorescence emission data for compounds **1**-**6**.

Compound	Solid State	Solution[a]	
	λ_{em} (nm)[b]	λ_{em} (nm)[b]	Φ_f (%)[c]
Me_3Ge-Ge(*p*-Tol)$_3$ (**1**)[d]	357, 373, 393 (300)	286(270)	3.27
Ph_3Sn-Ge($SiMe_3$)$_3$ (**2**)	398 (350)	335 (285)	0.93
Ph_3Ge-Ge(C_6F_5)$_3$ (**3**)	373 (270)	377 (265)	12.50
(*p*-Tol)$_3$Ge-$SiMe_2$-$SiMe_3$ (**4**)	400 (290), 427 (370)	331, 350 (275)	10.64
(*p*-Tol)$_3$Ge-$GeMe_2$-Ge(*p*-Tol)$_3$ (**5**)	438 (380)	338 (285)	1.85
(*p*-Tol)$_3$Ge-$SiMe_2$-$SiMe_3$-Ge(*p*-Tol)$_3$ (**6**)	416 (300), 445 (320)	363, 375 (260)	1.98

[a] Spectra were recorded in CH_2Cl_2. [b] Excitation wavelength (λ_{ex}, nm) shown in parentheses. [c] Quantum yield. [d] The data from the reference [9].

The fluorescence of compounds **1**–**6** in solution shows that the electronic properties of the substituents on the Ge atom significantly affect the Stokes shift and the quantum yield. Introduction of electron withdrawing groups resulted in a red shift with high quantum yield. In the case of the silyl substituted derivatives, **4** and **6**, two emission bands were observed, indicating several excitation fragments.

On contrary, in solid state, silyl substituted derivatives **4** and **6** showed only one fluorescence band. The emission wavelengths were red shifted due to the strong interaction between molecules inside the molecular crystal in comparison with the results previously obtained in solution.

The studies presented in earlier research[8] has shown that the "conductance" of a molecule in solution could be measured by using a complex scanning tunneling microscope technique based on the break-junction (STM-BJ). Nevertheless, measures obtained using this method are not representative of the physical properties of the bulk material. Most of the conductivity studies[6] carried on polysilanes (polygermanes) used time-resolved methods (such as FP-TRMC or TOF). Those studies have measured the intramolecular charge carrier mobility and conductivity without predicting the carrier transport properties for long distances in the bulk material, and thus having only limited significance.

In this work, the conductivity study was carried out by using DC and AC conductivity techniques, as well as photoconductivity methods. Compounds **1**–**6** were analyzed as pellets made from the polycrystalline powder for **1**-**4** and single crystals for **1**, **5** and **6**. Furthermore, the doping procedure by iodination was used for compound **6**. All of the studied compounds have shown resistance typical of dielectric materials and no photoconductivity was observed. When compared to published data[6d,8a,8b], our results tend to indicate that the charge carriers movements are hampered within the oligogermane molecules in the bulk material.

It is well known that the mobility of the charge carriers (usually holes in related compounds) strongly depends on the interfaces between molecules and between domains. In other words the conductivity is determined by the structure of the material and decreases when increasing the number of domain borders.[28] There could be several reasons that might explain the low bulk conductivity and photoconductivity of the studied materials. First possible reason is high energy barriers (either between molecules inside the material or at the contact point with the metallic electrodes) may be preventing the charge carriers from moving. Also, a high number of the recombination centers can be present within the material itself. Nevertheless, it is safe to assume that the conductivity could be improved by tweaking the oligogermanes. For instance introducing longer chain of σ-conjugated Group 14 atoms or introducing novel substituents (like thiomethyl groups[8a,8b]) on the Ge should improve the intermolecular electron transport and interaction with the electrodes and therefore this should result in observing an increase of the conductivity for these derivatives in the bulk material. Another way of solving this issue could be mixing the oligogermanes with an electron transporting materials such as fullerenes.[5]

To measure the level of HOMO (which correlates with oxidation potential) electrochemical investigations for compound **2**, **3**, **4** and **6** were carried out under standard conditions in dichloromethane containing [NBu_4][PF_6] (0.10 M) as supporting electrolyte. All data are referred to standard for organometallic compounds reference Fc/Fc^+. None of the compounds showed any cathodic reduction. Catenated aryl substituted Group 14 compounds are known to have irreversible oxidations[22,29] (equal to n-1 waves, where n is a E atoms quantity in the chain)[16] since the E-E bonds are rapidly consequentially cleaved when oxidized.[9,30] This is differed from alkyl substituted derivatives where only one oxidation wave is observed.

Compound **2** (Figure 10) showed a series of a very close *chemically*-irreversible anodic oxidations at, respectively, E_{pa} = 1.06, 1.20, 1.41 and 1.62 V *vs.* Fc/Fc^+ (approximately 1.55, 1.69, 1.90 and 2.11 V *vs.* Ag/AgCl).[31] In addition, **2** displays an important degree of *electrochemical* irreversibility. The measured E_{pa}-$E_{pa/2}$ value for the first oxidation of **2** is diagnostic of a slow charge transfer process with coefficient (β) of 0.30.[32] No re-reduction wave was observed during the back scan due to

rapid following up chemical reaction happening after the initial electron transfers (EC type).[33] Whilst the first anodic event could presumably be attributed to the oxidation of the Sn-Ge bond (when compared with 1.52 V *vs.* Ag/AgCl for (*p*-Tol)$_3$GeSnMe$_3$)[9] followed by the rapid cleavage of the formed radical-cation,[9] the subsequent oxidations encompass the oxidations of the decomposition products of the Sn-Ge radical cation as well as the Ge-Si bond oxidation. This anodic behavior differs significantly from what has been previously reported for the other branched Group 14 derivatives, where only one oxidation is observed.[30c,d]

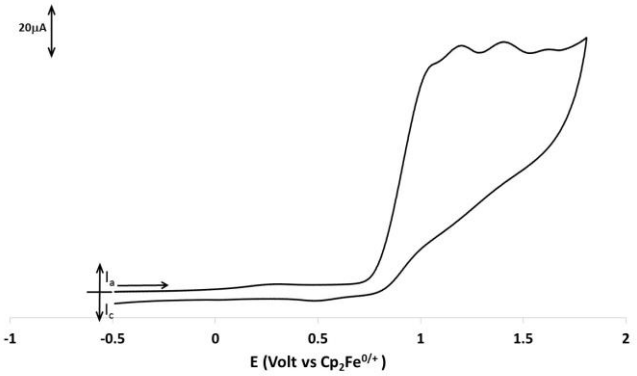

Figure 10. Cyclic voltammogram of 1mM **2** in dichloromethane - [NBu$_4$][PF$_6$] (0.1 M) solution. Sweeping rate 200 mV/s at room temperature.

The anodic electrochemistry of compounds **3** (Figure S19, Supporting Information) showed only one *chemically*-irreversible oxidation at E_{pa} = 1.62 V *vs.* Fc/Fc$^+$ (approximately 2.11 V *vs.* Ag/AgCl). The presence of electron withdrawing groups on the aromatic rings pushed the oxidation of the Ge-Ge bond to a very positive value and partially merges it with the solvent's wall, therefore no charge transfer coefficient could accurately be measured. The introduction of an electron withdrawing group within the core of **3** increases the oxidation potential by stabilizing the HOMO. Such a phenomenon is typically observed for oligogermanes containing a small number of element-element bonds.[10]

Compound **4** (Figure 11) displayed two successive *chemically*-irreversible oxidations at E_{pa} = 1.01, 1.30 V *vs.* Fc/Fc$^+$ (approximately 1.50, 1.79 V *vs.* Ag/AgCl). Again, the first oxidation displayed a slow electron transfer (β = 0.34). It is safe to assume that the first anodic event is due to the oxidation of the Ge-Si bond. The second oxidation is either due to the presence of a decomposition product resulting from the rapid cleavage of the Ge-Si radical-cation or to the oxidation of the Si-Si bond (when compared with 1.79 V *vs.* Ag/AgCl for (*p*-Tol)$_3$GeSiMe$_3$).[9] It is evident that elongation of the catenated atoms in the chain decreases the oxidation potentials (destabilizes the HOMO energy) and the introduction of aryl groups on the E atoms stabilize the radical-cation.

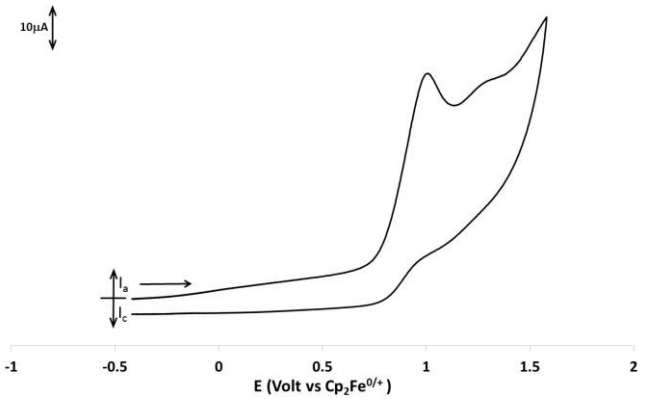

Figure 11. Cyclic voltammogram of 1 mM **4** in dichloromethane - [NBu$_4$][PF$_6$] (0.1 M) solution. Sweeping rate 200 mV/s at room temperature.

Compound **6** (Figure S20, Supporting Information) displayed a series of successive ill-defined *chemically*-irreversible oxidations. Three oxidations appear at E_{pa} = 0.99, 1.15 and 1.30 V *vs.* Fc/Fc$^+$ (approximately 1.48, 1.64 and 1.79 V *vs.* Ag/AgCl). Presumably, the first oxidation wave is due to the oxidation of the Ge-Si bond (when compared with 1.01 V for **4**). The oxidation potential is shifted to less positive value due to increased E-E chain length. The oxidation waves are too convoluted to allow measuring any charge transfer coefficient accurately. No significant improvement of the resulting was observed when the cyclic voltammetry experiments were conducted in dichloromethane containing the weakly coordinating salt [NBu$_4$][B(C$_6$F$_5$)$_4$] (0.05 M) as supporting electrolyte.[34]

The measured electrochemical data are in good agreement with what has been previously reported in the literature for similar compounds. Increasing the length of the catenated Group 14 atoms chain decreases the first oxidation potential (1.79 V *vs.* Ag/AgCl for (*p*-Tol)$_3$GeSiMe$_3$,[9] 1.50 V for **4** and 1.48 V for **6**); in addition, branching of the structure resulted in a smaller increase of the oxidation potential (1.06 V for **2** and 0.99 V for **6**).

Conclusions

We have disclosed new improved structure-semiconductor properties relationships for several oligogermanes as well as for several related silicon and tin compounds containing germanium atom. Although, the overall conductivity of the bulk material remains an issue, we are confident that this problem could be solved by doping the material, increasing the number of atoms in the catenated chain or by introducing functional groups (suitable for better interaction with the electrodes) on the germanium center.

We are confident that further studies on individual molecules similar to the ones reported in this work with known bulk (NMR, XRD, AEM) structure, optical (UV/vis, luminescence) and electrochemical properties (CV) will open new possibilities and will lead to new practical applications of catenated Group 14 compounds in the future.

Experimental Section

General methods and remarks. All operations with germanium derivatives were conducted in a dry argon atmosphere using standard Schlenk techniques. ^{1}H NMR (400.130 MHz), ^{13}C NMR (100.613 MHz), and ^{29}Si (79.495 MHz) NMR spectra were recorded on Bruker 400 or Agilent 400 spectrometers (at 295 K). Chemical shifts in the spectra are given in ppm relative to internal Me_4Si. Elemental analyses were carried out using HeraeusVarioElementar instrument. UV/visible spectra were recorded using two ray spectrophotometer Evolution 300 «Thermo Scientific» with cuvette of 0.10 cm long. Fluorescence (room temperature) spectra were recorded with Hitachi F-7000 spectrofluorimeter. Diffuse light scattering and adsorption was investigated with the use of LS-55 Perkin Elmer spectrophotometer. The surface structure of the obtained crystal was investigated using an atomic force microscope (AFM) "Multimode V" (Production Veeco) in tapping mode. DC conductivity and photoconductivity of the samples was measured with Keithley 6487 picoammeter. AC conductivity and photoconductivity was measured by NR 4192 impedance analyzer. Silver epoxy paste was used to produce electric contacts to the samples. For the photoconductivity measurements the samples were illuminated by 1 kW high pressure xenon lamp (with white spectrum) through MDR-12 monochromator. Mass spectra (EI-MS, 70 eV) were recorded on a quadropoule mass spectrometer FINNIGAN MAT INCOS 50 with direct insertion; all assignments were made with reference to the most abundant isotopes.

Solvents were dried by usual procedures. Diethyl ether were stored under solid KOH and then distilled under sodium/benzophenone. *n*-Hexane were refluxed and distilled over sodium. Dichloromethane was distilled over CaH_2. C_6D_6 was distilled over sodium under argon. $CDCl_3$ was distilled over CaH_2 under argon.

*n*BuLi (“Aldrich”), Me_3Si-Me_2SiCl (“Aldrich”), $ClMe_2Si$-Me_2SiCl (“Aldrich”) were the commercial reagents and were used as received. Compounds (*p*-Tol)$_3$GeH,[35] Me_4Ge,[9] (*p*-Tol)$_3$Ge-$GeMe_3$ (**1**),[9] Ph_3Sn-$Ge(SiMe_3)_3$ (**2**),[9] $(C_6F_5)_3$Ge-$GePh_3$ (**3**)[10] were synthesized according to literature procedures. Acetyl chloride was distilled over PCl_5 under flow of argon.

Dimethyldichlorogermane, Me_2GeCl_2. The improved procedure was used.[36] At 0°C under strong stirring acetyl chloride (51.00 mL, 56.50 g, 720.00 mmol) was added dropwise to the mixture of Me_4Ge (26.00 g, 200.00 mmol) and anhydrous $AlCl_3$ (112.00 g, 840.00 mmol). Reaction mixture was slowly warmed to room temperature and stirred for 5 h, then heated at 100°C for 1 h. Volatile materials were distilled twice using effective condenser, giving colorless liquid, b.p. 120-123 °C, b.p.124 °C.[37] Yield: 18.40 g (53%). ^{1}H NMR ($CDCl_3$, 400.130 MHz): δ 1.20 (s, 6H, CH_3). ^{13}C{^{1}H} NMR ($CDCl_3$, 100.613 MHz): δ 10.77 (CH_3).

Dimethyl(tris(*p*-tolyl)germyl)trimethylsilylsilane, (*p*-Tol)$_3$Ge-$SiMe_2$-$SiMe_3$ (4). *a) Synthesis of [tris(p-tolyl)germyl]lithium.* At room temperature solution of *n*BuLi in *n*-hexane (2.5 M, 0.46 mL, 1.15 mmol) was added dropwise to the solution of (*p*-Tol)$_3$GeH (0.40 g, 1.15 mmol) in ether (20 mL). Reaction mixture was stirred for 6 h. The solution of lithium compound was used further without purification.

*b) Synthesis of **3**.* Solution of Me_3Si-Me_2SiCl (0.24 mL, 1.15 mmol) in ether (20 mL) was added dropwise to the ethereal solution of (*p*-Tol)$_3$GeLi obtained as described above. Reaction mixture was stirred overnight. Then water (20 mL) was added, water phase was extracted with ether (3x20 mL), combined organic phases were dried over anhydrous Na_2SO_4. All volatile materials were removed under reduced pressure. Residue was recrystallized from *n*-hexane. Compound **4** was isolated as a white microcrystal material, m.p. 80-81 °C. Yield: 0.32 g, 58%. ^{1}H NMR ($CDCl_3$, 400.130 MHz): δ 7.32 (d, 6H, $^{3}J_{H\text{-}H}$ = 7.8 Hz, *p*-C_6H_4), 7.14 (d, 6H, $^{3}J_{H\text{-}H}$ = 7.8Hz, *p*-C_6H_4), 2.35 (s, 9H, *p*-$C_6H_4CH_3$), 0.33 (s, 6H, $^{2}J_{H\text{-}29Si}$ = 3.1 Hz, $SiMe_2$), -0.01 (s, 9H, $^{2}J_{H\text{-}29Si}$ = 3.1 Hz, $SiMe_3$). ^{13}C{^{1}H} NMR ($CDCl_3$, 100.613 MHz): δ 137.78 (2 *ipso*-C_6H_4), 135.34, 128.87 (*p*- and *m*-C_6H_4) (aromatic carbons), 21.41 (*p*-$C_6H_4CH_3$), -1.46 ($SiMe_2$), -4.56 ($SiMe_3$). Two *ipso* aromatic carbon atoms are overlapped. ^{29}Si NMR ($CDCl_3$, 79.495 MHz): δ -15.36 ($SiMe_3$), -38.94 ($SiMe_2$). MS (EI, %): 477 ([M$^+$], 17), 462 ([M – Me]$^+$, 4), 404 ([M – $SiMe_3$]$^+$, 11), 346 ([Tol$_3$Ge]$^+$, 100), 313 ([M – $SiMe_3$ – Tol]$^+$, 16), 255 ([Tol$_2$Ge]$^+$, 41), 165 ([TolGe + H]$^+$, 17), 131 ([Si_2Me_5]$^+$, 12). UV (CH_2Cl_2), λ_{max}, nm (ε, M^{-1} cm^{-1}): 241 (2.5×10^4). Elemental analysis Calc. for $C_{26}H_{36}GeSi_2$ (477.345): C 65.42, H 7.60. Found: C 65.24, H 7.49.

2,2-Dimethyl-1,1,1,3,3,3-hexakis(*p*-tolyl)trigermane, (*p*-Tol)$_3$Ge-$GeMe_2$-Ge(*p*-Tol)$_3$ (5). Solution of Me_2GeCl_2 (0.20 mL, 1.69 mmol) in ether (20 mL) was added dropwise to the ethereal solution of (*p*-Tol)$_3$GeLi obtained as described above from (*p*-Tol)$_3$GeH (1.17 g, 3.37 mmol) and *n*BuLi in *n*-hexane (2.5 M, 1.35 ml, 3.37 mmol). Reaction mixture was stirred overnight. Then water (20 mL) was added, water phase was extracted with ether (3x20 mL), combined organic phases were dried over anhydrous Na_2SO_4. All volatile materials were removed under reduced pressure. Residue was recrystallized from the mixture of *n*-hexane/dichloromethane. Compound **5** was isolated as a white powder, m.p. 205-206°C. Yield: 1.12 g, 84%. ^{1}H NMR ($CDCl_3$, 400.130 MHz): δ 7.18 (d, 12H, $^{3}J_{H\text{-}H}$ = 7.8 Hz, *p*-$C_6H_4CH_3$), 7.03 (d, 12H, $^{3}J_{H\text{-}H}$ = 7.8 Hz, *p*-$C_6H_4CH_3$), 2.35 (s, 18H, *p*-$C_6H_4CH_3$), 0.59 (s, 6H, $GeMe_2$). ^{13}C{^{1}H} NMR ($CDCl_3$, 100.613 MHz): δ 137.91, 134.65 (2 *ipso*-$C_6H_4CH_3$-*p*), 135.45, 128.87 (*p*- and *m*-$C_6H_4CH_3$) (aromatic carbons), 21.35 (*p*-$C_6H_4CH_3$), -2.14 ($GeMe_2$). MS (EI, %): 795 ([M$^+$], 3), 780 ([M – Me]$^+$, 2), 449 ([M – $GeTol_3$]$^+$, 9), 346 ([Tol$_3$Ge]$^+$, 100), 255 ([Tol$_2$Ge]$^+$, 21), 165 ([TolGe + H]$^+$, 14). UV (CH_2Cl_2), λ_{max}, nm (ε, M^{-1} cm^{-1}): 251 (4.0×10^4). Elemental analysis calc. for $C_{44}H_{48}Ge_3$ (794.6819): C 66.50, H 6.09. Found: C 66.40, H 6.03.

1,1,2,2-Tetramethyl-1,2-bis[tris(*p*-tolyl)germyl]disilane, (*p*-Tol)$_3$Ge-$SiMe_2$-$SiMe_2$-Ge(*p*-Tol)$_3$ (6). Solution of $ClMe_2Si$-Me_2SiCl (0.12 mL, 0.64 mmol) in ether (20 mL) was added dropwise to the ethereal solution of (*p*-Tol)$_3$GeLi obtained as described above from (*p*-Tol)$_3$GeH (0.45 g, 1.30 mmol) and *n*BuLi in *n*-hexane (2.5 M, 0.52 ml, 1.30 mmol). Reaction mixture was stirred overnight. Then water (20 mL) was added, water phase was extracted with ether (3x20 mL), combined organic phases were dried over anhydrous Na_2SO_4. All volatile materials were removed under reduced pressure. Residue was recrystallized from the mixture of *n*-hexane/dichloromethane. Compound **6** was isolated as a white powder, m.p. 233-234 °C. Yield: 0.32 g, 68%. ^{1}H NMR ($CDCl_3$, 400.130 MHz): δ 7.32 (d, 12H, $^{3}J_{H\text{-}H}$ = 7.8 Hz, *p*-$C_6H_4CH_3$), 7.15 (d, 12H, $^{3}J_{H\text{-}H}$ = 7.8 Hz, *p*-C_6H_4), 2.37 (s, 18H, *p*-$C_6H_4CH_3$), 0.23 (s, 12H, $SiMe_2$). ^{13}C{^{1}H} NMR ($CDCl_3$, 100.613 MHz): δ 137.89, 135.22 (2 *ipso*-$C_6H_4CH_3$), 135.36, 128.93 (*p*- and *m*-$C_6H_4CH_3$) (aromatic carbons), 21.40 (*p*-$C_6H_4CH_3$), -3.03 ($SiMe_2$). ^{29}Si NMR ($CDCl_3$, 79.495 MHz): δ -34.66 ($SiMe_2$). MS (EI, %): 809 ([M$^+$], 1), 687 ([M – 2Me - Tol]$^+$, 1), 462 ([M – $GeTol_3$]$^+$, 41), 346 ([Tol$_3$Ge]$^+$, 100), 405 ([Tol$_3$GeSiMe_2]$^+$, 2), 255 ([Tol$_2$Ge]$^+$, 10). UV

(CH_2Cl_2), λ_{max}, nm (ε, M^{-1} cm^{-1}): 258 (4.7×10^4). Elemental analysis calc. for $C_{46}H_{54}Ge_2Si_2$ (808.312): C 68.35, H 6.73. Found: C 68.23, H 6.68.

Electrochemistry. Electrochemical measurements were carried out using an Autolab 302N potentiostat interfaced through Nova 2.0 software to a personal computer. Electrochemical measurements were performed in a glovebox under oxygen levels of less than 5 ppm using solvent that had been purified by passing through an alumina-based purification system. Diamond-polished glassy carbon electrodes of 3 mm diameter were employed for cyclic voltammetry (CV) scans. CV data were evaluated using standard diagnostic criteria for diffusion control and for chemical and electrochemical reversibility. The experimental reference electrode was a silver wire coated with anodically deposited silver chloride and separated from the working solution by a fine glass frit. The electrochemical potentials in this paper are referenced to ferrocene/ferrocenium couple, as recommended elsewhere.[38] The ferrocene potential was obtained by its addition to the analyte solution.[39] At an appropriate time in the experiment $[NBu_4][B(C_6F_5)_4]$ was prepared as previously described.[40]

X-ray crystallography. Experimental intensities were measured on a STADIVARI Pilatus (for **5** and **6**) diffractometer using ω-scan mode. Absorption correction based on measurements of equivalent reflections was applied. The structures were solved by direct methods and refined by full matrix least-squares based on F^2 with anisotropic thermal parameters for all non-hydrogen atoms. All aromatic hydrogen atoms were placed in calculated positions. All H atoms were refined using a riding model. Details of X-ray studies are given in Table S1 (Supporting Information).

Crystallographic Data Centre as supplementary publications under the CCDC numbers 1510022-1510023. This information may be obtained free of charge from the Cambridge Crystallographic Data Centre via www.ccdc.cam.ac.uk/data_request/cif.

Acknowledgements

This work was financially supported by the Russian President Grant for Young Russian Scientists (MK-1790.2014.3 - KVZ), in part by M.V. Lomonosov Moscow State University Program of Development (KVZ), Nazarbayev University (ORAU grant for Medicinal Electrochemistry - KL) and the Ministry of Education and Science of Kazakhstan (KL).

Keywords: oligogermanes • silagermanes • luminescence • organic semiconductor • X-ray analysis

[1] a) R. D. Miller, J. Michl, *Chem. Rev.* **1989**, *89*, 1359-1410; b) J. M. Zeigler, *Synth. Met.* **1989**, *28*, 581-591.

[2] a) C. Marschner, J. Hlina, in *Comprehensive Inorganic Chemistry II (Second Ed.)* (Eds.: J. Reedijk, K. Poeppelmeier), Elsevier, Amsterdam, **2013**, pp. 83-117; b) M. L. Amadoruge, C. S. Weinert, *Chem. Rev.* **2008**, *108*, 4253-4294.

[3] a) H. Teruyuki, U. Yuko, R. N. Prabhakar, T. Masato, *Chem. Lett.* **1992**, *21*, 647-650; b) R. West, *J. Organomet. Chem.* **1986**, *300*, 327-346.

[4] a) M. Abkowitz, M. Stolka, *Solid State Commun.* **1991**, *78*, 269-271; b) M. Abkowitz, M. Stolka, *J. Non-Cryst. Solids* **1989**, *114,* 342-344; c) Y. Kunimi, S. Seki, S. Tagawa, *Solid State Commun.* **2000**, *114*, 469-472; d) K. Mochida, S.-S. Nagano, *Inorg. Chem. Commun.* **1998**, *1*, 289-291.

[5] A. Feigl, A. Bockholt, J. Weis, B. Rieger, in *Silicon Polymers* (Ed.: M. A. Muzafarov), Springer Berlin Heidelberg, Berlin, Heidelberg, **2011**, pp. 1-31.

[6] a) R. West, L. D. David, P. I. Djurovich, K. L. Stearley, K. S. V. Srinivasan, H. Yu, *J. Am. Chem. Soc.* **1981**, *103*, 7352-7354; b) K. Mochida, S. Maeyama, M. Wakasa, H. Hayashi, *Polyhedron* **1998**, *17*, 3963-3967; c) S. Shu, A. Anjali, K. Yoshiko, S. Akinori, T. Seiichi, M. Kunio, *Chem. Lett.* **2005**, *34*, 1690-1691; d) A. Acharya, S. Seki, A. Saeki, S. Tagawa, *Synth. Met.* **2006**, *156*, 293-297; e) S. Seki, A. Saeki, A. Acharya, Y. Koizumi, S. Tagawa, K. Mochida, *Radiat. Phys. Chem* **2008**, *77*, 1323-1327.

[7] S. Nešpůrek, A. Eckhardt, *Polym. Adv. Technol.* **2001**, *12*, 427-440.

[8] a) R. S. Klausen, J. R. Widawsky, M. L. Steigerwald, L. Venkataraman, C. Nuckolls, *J. Am. Chem. Soc.* **2012**, *134*, 4541-4544; b) T. A. Su, H. Li, V. Zhang, M. Neupane, A. Batra, R. S. Klausen, B. Kumar, M. L. Steigerwald, L. Venkataraman, C. Nuckolls, *J. Am. Chem. Soc.* **2015**, *137*, 12400-12405; c) T. A. Su, H. Li, R. S. Klausen, J. R. Widawsky, A. Batra, M. L. Steigerwald, L. Venkataraman, C. Nuckolls, *J. Am. Chem. Soc.* **2016**, *138*, 7791-7795.

[9] K. V. Zaitsev, E. K. Lermontova, A. V. Churakov, V. A. Tafeenko, B. N. Tarasevich, O. K. Poleshchuk, A. V. Kharcheva, T. V. Magdesieva, O. M. Nikitin, G. S. Zaitseva, S. S. Karlov, *Organometallics* **2015**, *34*, 2765-2774.

[10] K. V. Zaitsev, A. A. Kapranov, A. V. Churakov, O. K. Poleshchuk, Y. F. Oprunenko, B. N. Tarasevich, G. S. Zaitseva, S. S. Karlov, *Organometallics* **2013**, *32*, 6500-6510.

[11] S. Roller, D. Simon, M. Drager, *J. Organomet. Chem.* **1986**, *301*, 27-40.

[12] M. Drager, D. Simon, *J. Organomet. Chemi.* **1986**, *306*, 183-192.

[13] K. Haberle, M. Drager, *J. Organomet. Chem.* **1986**, *312*, 155-165.

[14] M. Weidenbruch, A. Hagedorn, K. Peters, H. G. von Schnering, *Chem. Ber.* **1996**, *129*, 401-404.

[15] M. Weidenbruch, A. Hagedorn, K. Peters, H. G. von Schnering, *Angew. Chem., Int. Ed. Engl.* **1995**, *34*, 1085-1086.

[16] M. L. Amadoruge, E. K. Short, C. Moore, A. L. Rheingold, C. S. Weinert, *J. Organomet. Chem.* **2010**, *695*, 1813-1823.

[17] J. Hlina, R. Zitz, H. Wagner, F. Stella, J. Baumgartner, C. Marschner, *Inorg. Chim. Acta* **2014**, *422*, 120-133.

[18] a) C. S. Weinert, *Dalton Trans.* **2009**, 1691-1699; b) C. Marschner, J. Baumgartner, A. Wallner, *Dalton Trans.* **2006**, 5667-5674.

[19] J. Fischer, J. Baumgartner, C. Marschner, *Organometallics* **2005**, *24*, 1263-1268.

[20] H. Wagner, J. Baumgartner, T. Müller, C. Marschner, *J. Am. Chem. Soc.* **2009**, *131*, 5022-5023.

[21] M. Shimizu, S. Ishizaki, H. Nakagawa, T. Hiyama, *Synlett* **1999**, *1999*, 1772-1774.

[22] M. Okano, K. Mochida, *Chem. Lett.* **1990**, 701-704.

[23] H. Gilman, W. H. Atwell, P. K. Sen, C. L. Smith, *J. Organomet. Chem.* **1965**, *4*, 163-167.

[24] A. Castel, P. Riviere, B. Saintroch, J. Satge, J. P. Malrieu, *J. Organomet. Chem.* **1983**, *247*, 149-160.

[25] E. K. Schrick, T. J. Forget, K. D. Roewe, A. C. Schrick, C. E. Moore, J. A. Golen, A. L. Rheingold, N. F. Materer, C. S. Weinert, *Organometallics* **2013**, *32*, 2245-2256.

[26] W. Fa, X. C. Zeng, *Chem. Commun.* **2014**, *50*, 9126-9129.

[27] K. Takeda, H. Teramae, N. Matsumoto, *J. Am. Chem. Soc.* **1986**, *108*, 8186-8190.

[28] S. S. Lee, C. S. Kim, E. D. Gomez, B. Purushothaman, M. F. Toney, C. Wang, A. Hexemer, J. E. Anthony, Y.-L. Loo, *Adv. Mater.* **2009**, *21*, 3605-3609.

[29] K. Mochida, C. Hodota, R. Hata, S. Fukuzumi, *Organometallics* **1993**, *12*, 586-588.

[30] a) M. L. Amadoruge, J. R. Gardinier, C. S. Weinert, *Organometallics* **2008**, *27*, 3753-3760; b) C. R. Samanamu, M. L. Amadoruge, A. C. Schrick, C. Chen, J. A. Golen, A. L. Rheingold, N. F. Materer, C. S. Weinert, *Organometallics* **2012**, *31*, 4374-4385; c) C.R. Samanamu, M. L. Amadoruge, C. H. Yoder, J. A. Golen, C. E. Moore, A. L. Rheingold, N. F. Materer, C. S. Weinert, *Organometallics* **2011**, 1046-1058; d) C.R. Samanamu, N. F. Materer, C. S. Weinert, *J. Organomet. Chem.* **2012**, 62-65.

[31] In practical terms, electrochemical reversibility (also termed Nernstian behavior) refers to the speed of charge-transfer in a redox reaction, whereas chemical reversibility refers to follow-up reactions that accompany the charge-transfer process. For an introductory discussion of these terms, see Bard, A. J.; Faulkner, L. N., *Electrochemical Methods*, John Wiley & Sons, New York, **2001**, 2nd Ed., pp 35-38 and pp 44-49.

[32] a) A. J. Bard, L. N. Faulkner, *Electrochemical Methods,* John Wiley & Sons, New York, **2001**, 2nd Ed., pp 35-38 and pp 236; b) D. A. Dickie, B. E. Chacon, A. Issabekov, K. Lam, R. A. Kemp, *Inorg. Chim. Acta* **2016**, *453*, 42-50.

[33] D. H. Evans, *Chem. Rev.* **1990**, *90*, 739-751.
[34] K. Lam, W. E. Geiger, *J. Org. Chem.* **2013**, *78*, 8020-8027.
[35] V. Y. Lee, H. Yasuda, M. Ichinohe, A. Sekiguchi, *J. Organomet. Chem.* **2007**, *692*, 10-19.
[36] H. Sakurai, K. Tominaga, T. Watanabe, M. Kumada, *Tetrahedron Lett.* **1966**, *7*, 5493-5497.
[37] H. Schumann, L. Esser, J. Loebel, A. Dietrich, D. Van der Helm, X. Ji, *Organometallics* **1991**, *10*, 2585-2592.
[38] G. Gritzner, J. Kuta, *Pure Appl. Chem.* **1984**, *56*, 461-466.
[39] R. R. Gagne, C. A. Koval, G. C. Lisensky, *Inorg. Chem.* **1980**, *19*, 2854-2855.
[40] K. Lam, W. E. Geiger, *J. Organomet. Chem.* **2016**, *817*, 15-20.